


## The assessment of the effectiveness of the unimodal and bimodal models to evaluate the water flow through nature-based solutions substrates

Michele Turco <sup>\*</sup>, Stefania Anna Palermo, Ada Polizzi, Ludovica Presta, Behrouz Pirouz and Patrizia Piro

Department of Civil Engineering, University of Calabria, 87036 Rende (CS), Italy

<sup>\*</sup>Corresponding author. E-mail: michele.turco@unical.it

 MT, 0000-0003-3768-842X

### ABSTRACT

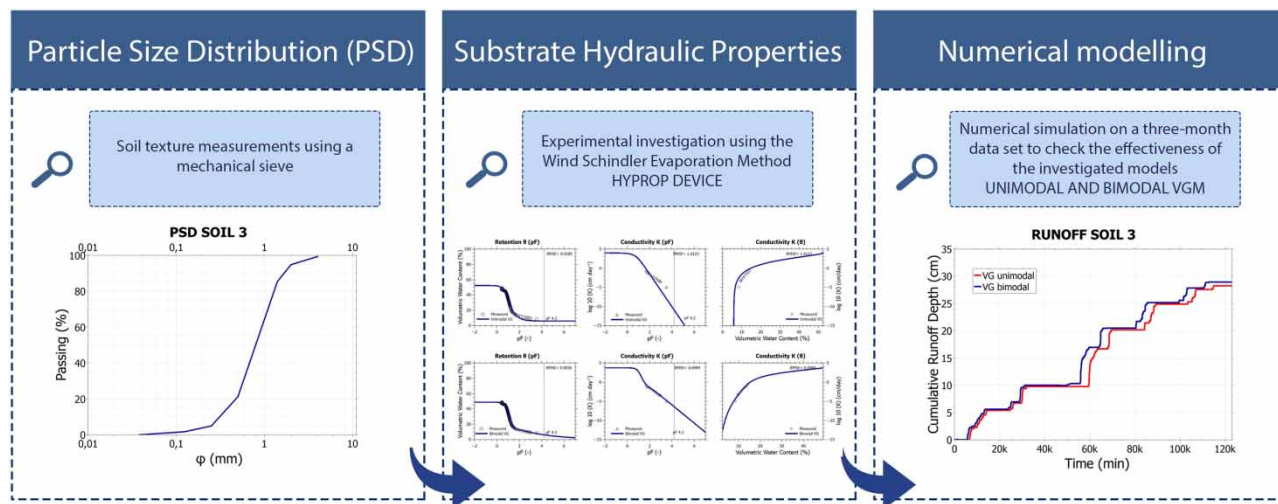
Nature-based solutions are popular techniques for managing stormwater. Most of them allow porous media as their main layer. The description of the Soil Water Retention Curve (SWRC) as the Unsaturated Hydraulic Conductivity Curve (UHCC) is often required to run the hydrological simulations with the physically based models. Using the unimodal and bimodal models to assess the SWRC and UHCC of soils is a widespread technique but their evaluation is often present in literature only in terms of curve fitting. Based on these assumptions, this work presents the performance assessment of the van Genuchten unimodal and bimodal models by functional evaluation of them based on the runoff from several substrates. Four substrates were investigated to define the structure, the SWRC, and the UHCC. Results showed that all substrates had a bimodal behaviour with lowest values of RMSE ( $RMSE_{\theta} = 0.0023$  to  $0.0037$ ,  $RMSE_K = 0.0636$  to  $0.1284$ ). Finally, a numerical simulation using the HYDRUS-1D model was performed for a three-month data set to check the effectiveness of the unimodal model instead of the bimodal one. The findings have shown that the unimodal model must be preferred instead of the bimodal because it has fewer parameters and assured low discrepancies in runoff volume ( $\epsilon = 0.00\%$  to  $6.25\%$ ).

**Key words:** HYDRUS-1D, nature-based solution, physically based model, SWRC, UHCC, van Genuchten models

### HIGHLIGHTS

- The aim of the work is to check the effectiveness of the unimodal and bimodal models to predict runoff volume from NBS substrates.
- Experimental investigation on four soil substrates to define their hydraulic behaviour.
- Numerical simulations to assess the performances of the two investigated models.
- The benefit of using unimodal model instead bimodal was assessed.

### GRAPHICAL ABSTRACT



This is an Open Access article distributed under the terms of the Creative Commons Attribution Licence (CC BY-NC-ND 4.0), which permits copying and redistribution for non-commercial purposes with no derivatives, provided the original work is properly cited (<http://creativecommons.org/licenses/by-nc-nd/4.0/>).

## NOMENCLATURE

$\varphi$	diameter (L)
$p_d$	dry weight (M)
Cu	coefficient of uniformity (-)
$d_{60}$	diameters corresponding to the passing percentage of 60 (L)
$d_{10}$	diameters corresponding to the passing percentage of 10 (L)
$\theta$	volumetric water content ( $L^3 L^{-3}$ )
$t$	time (T)
$q$	volumetric flux density ( $L T^{-1}$ )
$h$	substrate water matric head (L)
$K$	hydraulic conductivity ( $L T^{-1}$ )
$z$	vertical axis (L)
$\theta_S$	saturation water content ( $L^3 L^{-3}$ )
$\theta_r$	residual water content ( $L^3 L^{-3}$ )
$S$	the sink term (L)
$\alpha$	inverse of pressure head at air-entry pressure head ( $L^{-1}$ )
$n$	shape parameters associated with the distribution of pores (-)
$m$	shape parameters associated with the distribution of pores in the soil (-)
$\tau$	tortuosity parameter (-)
$w_i$	weight associated with the order of voids (-)
$V_{r,VGU}$	total volume runoff obtained defining the flow domain with the use of the VG unimodal model (L)
$V_{r,VGB}$	total volume runoff obtained defining the flow domain with the use of the VG bimodal model (L)
$\varepsilon$	relative percentage error (%)

## 1. INTRODUCTION

In recent decades, urban drainage systems have been overloaded by the combined effects of urbanization and climate change. Urbanization causes soil's waterproofing that modifies the natural hydrological cycle due to the reduction of hydrological losses: in this way, in urban basins total volume runoff and peak flow increases (Arnold & Gibbons 1996; Finkenbine *et al.* 2000; Rose & Peters 2001), peak flow lag time reduces (Espey *et al.* 1964) and water quality gets worse (Leopold 1968; Fletcher *et al.* 2013; Kumar & Singh 2023). Climate changes derive from global warming and make extreme meteoric events, such as heavy precipitations, drought and heat waves, increasingly frequent (Palermo *et al.* 2019; Masson-Delmotte *et al.* 2021; Penny *et al.* 2023). In particular, the rise of heavy precipitations involves the sewer system's crisis due to exceeding the drainage capacity and increases the likelihood of urban pluvial flooding (Falconer *et al.* 2009). Recently, the scientific community has focused its attention to the nature-based solutions (NBS) to mitigate the effects of urbanization and climate changes in stormwater management. NBS consists of a series of techniques that restore the hydrological cycle by reproducing natural processes, such as infiltration, filtration, retention, detention and evaporation. Among these solutions, the most popular are green roofs, green walls, permeable pavements, bioretention systems and detention basins. Based on the principle of hydraulic and hydrological invariance, their distribution within an urban basin allows the partial restoration of the pre-urban hydrological cycle: in this way, the runoff volumes are controlled and the peak flows are reduced (Carbone *et al.* 2014; Turco *et al.* 2018; Palermo *et al.* 2020; Wang *et al.* 2021; Kumar & Singh 2023), the basin response times are delayed (Stovin *et al.* 2017; Salerno *et al.* 2021) and the concentration of pollutants can be reduced (Monterusso *et al.* 2004; Masi *et al.* 2016; Pirouz *et al.* 2020; Turco *et al.* 2020; Costa-Conceicao *et al.* 2023).

Several studies in the literature have shown that the ability of NBS to control the runoff volumes and the peak flows depends on the hydraulic properties of the soil substrate (Brunetti *et al.* 2016; Sims *et al.* 2019; Turco *et al.* 2022), in particular by the definition of the soil water retention curve (SWRC) and the unsaturated hydraulic conductivity curve (UHCC). The functions are influenced by soil's physical characteristics, in terms of texture (Wösten *et al.* 1995; Schaap & Leij 1998), which consists of the particle composition divided into gravel, sand, silt and clay fractions, and in terms of structure (Vervoort & Cattle 2003; Kutlílek 2004), that represents the particles' aggregation mode. Furthermore, several studies have shown that soil texture influences its structure: in fact, soils with a very homogeneous particle size composition (PSC) have a single family of small pores that develop between solid particles; on the other side, soils with a heterogeneous composition present a double order of pores of different sizes, i.e. the micro-pores, called intra-aggregate, are those that develop within the structure of the aggregate, and the macro-pores, called inter-aggregate, are those that develop between one aggregate and another

(Brewer 1965; Hadas 1987; Dexter 1988; Oades & Waters 1991; Dexter *et al.* 2008). In this way, soil with a single porosity system has a unimodal hydraulic behaviour, while soils with a dual porosity system, in which micro-pores and macro-pores have different permeability, have bimodal hydraulic behaviours (Ross & Smettem 1993; Durner 1994). The unimodal and bimodal soil hydraulic behaviours can be studied with specific literature parametric models such as the traditional unimodal constrained van Genuchten–Mualem model (Mualem 1976; van Genuchten 1980) and the bimodal constrained van Genuchten model (Durner 1994) and their use in the literature is very widespread.

Thus, Zhang *et al.* (2022) have analysed the effects of pore-size distribution on pedo-transfer functions (PTF). They used 192 noted soil samples, whose retention and unsaturated conductivity data are made available by three databases for PTF development, i.e. unsaturated soil hydraulic database (UNSODA 2.0), Vereecken and European HYdropedological Data Inventory (EU-HYDI); soil texture information was available only on 79 samples. The PTF data have been interpolated with both van Genuchten unimodal and van Genuchten bimodal models using different fitting strategies in order to define the optimal soil hydraulic parameters. Considering the best strategy (the one having the lowest AIC index) for the 64.9% of soil samples, the joint fitting of retention data conductivity data represents the best statistical strategy to achieve optimal soil hydraulic parameters; in addition, the bimodality is not limited to fine-textured soil, but shown up also in coarse-textured soils.

Moreover, the difference between unimodal and bimodal hydraulic models is not only reflected in the fitting quality of retention and unsaturated conductivity data with the theoretical SWRC and UHCC but also in the response of the soil to medium and long-term hydrological processes as shown by Coppola *et al.* (2009). In this study, different soil samples have been analysed with retention laboratory measurements and conductivity field measurements, and then the SWRC and the UHCC have been defined using unimodal and bimodal models.

In terms of fitting quality, the parametric models are both effective, but the differences between them emerge during the 1D vertical infiltration Monte Carlo simulation because the bimodal model simulation was more representative to reproduce the water content during heavy precipitations.

However, as shown by Coppola (2000), a better quality curve fitting using a bimodal model in the case of a dual porosity soil is associated with the definition of a huge number of parameters, which often have a high correlation. In this way, using a bimodal hydraulic model can increase the uncertainty because the degree of correlation between the unknown parameters increases.

Based on these considerations, we want to investigate the performances of the van Genuchten unimodal and bimodal models by functional evaluation of them based on the runoff from NBS substrates proposing a simple approach, starting from the experimental analysis to classify the hydraulic behaviour of the media investigated then using a simple hydrological simulation to evaluate which model should be preferred with low discrepancies in the results. So, this work will suggest experimental and mathematical procedures to study both the texture of the soils investigated both their hydraulic behaviour which consists of (a) experimental investigation to define the particle size distribution (PSD) of the soils; (b) experimental analysis of a method to define the SWRC and the UHCC of the substrates investigated; (c) a long-term simulation with the van Genuchten unimodal and bimodal models to assess the runoff volume from the system using the HYDRUS-1D model.

## 2. THEORY AND METHODS

### 2.1. Particle size distribution

The PSD is a measurement of soil texture and it is the frequency diagram cumulative weight percentages of particles classified by diameter ( $\varphi$ ) in clay ( $\varphi < 0.002$  mm), silt ( $0.002$  mm  $< \varphi < 0.06$  mm), sand ( $0.06$  mm  $< \varphi < 2$  mm) and gravel ( $\varphi > 2$  mm). Following the Standard Test Methods for PSD of ASTM D6913, the PSD has been obtained by sieving the coarse fraction of the soil sample, made of particles having a diameter  $\varphi \geq 0.038$  mm, previously dried in the oven at 105 °C for 24 h. The soil sample has been placed in the mechanical sieve and then each sieve has retained the solid particles having a diameter greater than or equal to that of the opening of its meshes.

The choice of sieves to be used depends on the characteristics of the soil: for Soil 1 and Soil 4 standard sieves with a diameter of 10, 5.6, 4, 2, 1, 0.5, 0.125, 0.063 and 0.038 mm have been used, while for Soil 2 and Soil 3 standard sieves with a diameter of 4, 2, 1.4, 1, 0.5, 0.25, 0.125, 0.063 and 0.038 mm have been used.

Thus, the sample dry weight ( $p_d$ ) was defined as well as the weight of the solid fraction from each sieve ( $p(\varphi)$ ). Finally, the passing percentage of each sieve has been calculated using Equation (1):

$$\text{passing } (\varphi) = \left( \frac{p_d - p(\varphi)}{p_d} \right) \cdot 100 \tag{1}$$

To track the PSD, the experimental points ( $\varphi$ ; passing  $(\varphi)$ ) referring to sieves have been reported in a graph, where the diameter's logarithm is reported along the horizontal axis and the passing percentage is reported along the vertical axis (Figure 1). From the PSD (Table 1), graphically the PSC has been obtained, knowing the intervals of the different particle size fractions, and the coefficient of uniformity  $C_u$  has been defined as a parameter of the degree of an assortment of the particles (2):

$$C_u = \frac{d_{60}}{d_{10}} \tag{2}$$

where  $d_{60}$  and  $d_{10}$  are the diameters corresponding, respectively, to the passing percentage of 60 and 10 obtainable graphically.

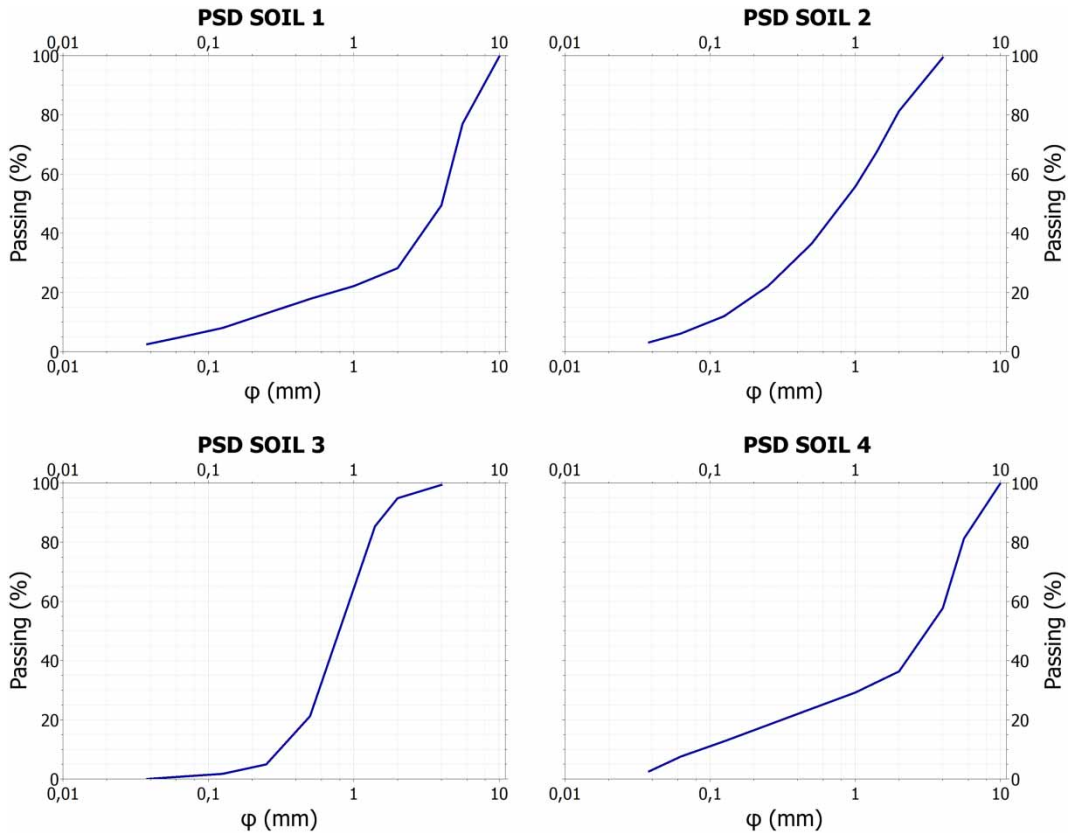


Figure 1 | Particle size distribution (PSD) of Soil 1, Soil 2, Soil 3 and Soil 4.

Table 1 | Summarize of the boundary and initial conditions

Boundary conditions	Initial conditions
Upper boundary condition ( $Z = L$ ): Atmospheric	$t = 0$ , constant matrix suction: $-100$ cm
Lower boundary condition ( $Z = 0$ ): Seepage face	

The higher the coefficient of uniformity, higher is the heterogeneity of the composition, in agreement with ASTM Standard D2487 (ASTM D2487 2000): if  $C_u \leq 2$  the soil is uniform,  $2 < C_u \leq 4$  the soil is poorly graduated,  $4 < C_u < 6$  the soil is well graduated and  $C_u \geq 6$  the soil is very well graduated.

## 2.2. Substrate hydraulic properties

The water flow through the unsaturated porous medium is much more complex compared to what happens in saturated soil because filtration develops through pores that are only partially filled entirely by water. It is determined by the gravitational, capillary and viscous resistance forces and it is governed by the continuity Equation (3) and the Darcy–Buckingham law (4):

$$\frac{\partial \theta}{\partial t} = \frac{\partial q_i}{\partial z_i} \quad (3)$$

$$q = -K(\theta) \frac{\partial h}{\partial z} \quad (4)$$

where  $\theta$  is the volumetric water content ( $L^3 L^{-3}$ ),  $t$  is the time (T),  $q$  is the volumetric flux density ( $L T^{-1}$ ),  $h$  is the substrate water matric head (L),  $K$  is the hydraulic conductivity ( $L T^{-1}$ ) and  $z$  is the vertical axis (L).

From their combination is obtained the Richards equation (Richards 1931), that is a nonlinear partial differential equation (Equation (5)):

$$\frac{\partial \theta}{\partial t} = \frac{\partial}{\partial z} \left[ K(\theta) \frac{\partial h}{\partial z} - 1 \right] \quad (5)$$

This equation used for water flow modelling in the unsaturated condition requires the knowledge of water retention function (SWRC) and the hydraulic conductivity function (UHCC). To assess the SWRC and UHCC, the HYPROP device was used (METER 2015). This fully automated measuring and evaluation device reproduces a wide method used in the literature, the evaporation method, developed by Wind (1969) and modified by Schindler (1980), which allows to assess soil moisture and pressure head over an evaporation process. Several simplifications of this method are also described in Peters & Durner (2008) and Schindler *et al.* (2010a, 2010b). To carry out the test, at the beginning, the sample has been saturated by capillarity and the device and the tensiometers have been refilled; later, the tensiometers have been screwed in, the saturated sample has been attached to the device and finally the mounted device has been placed on a digital scale.

During the test, the tensiometers measured the matrix potential of the soil water, while the balance measured the soil weight. Starting from these measures the HYPROP device has derived the experimental points of the SWRC and UHCC: the first one represents the trend of dimensionless water content  $\Theta$  ( $\Theta = \theta - \theta_r / \theta_s - \theta_r$ ) where  $\theta_s$  is the saturation water content ( $L^3 L^{-3}$ ) and  $\theta_r$  is the residual water content ( $L^3 L^{-3}$ ) versus matrix potential  $h(L)$ , while the second one represents the trend of hydraulic conductivity  $K$  ( $L T^{-1}$ ) versus matrix potential  $h$  (L) (or  $K$  versus  $\Theta$ ).

Finally, the experimental points have been interpolated by theoretical curves from van Genuchten unimodal and bimodal models using the HYPROP-FIT software (Pertassek *et al.* 2015).

## 2.3. Numerical modelling

A three-month data set (from January 2016 to March 2016) was used to perform the hydrological simulation. The data set was recorded from a weather station located at University of Calabria and it included wind velocity, atmospheric pressure, humidity, temperature, global solar radiation and precipitation. Based on the results achieved from the experimental investigations of SWRC about the best choice of the hydraulic behaviour of the four soils investigated (unimodal or bimodal), a numerical analysis was carried out using the HYDRUS-1D model (Šimůnek *et al.* 2016) to check the response of substrate to real precipitation: the objective is to establish whether the chosen theoretical model is the most convenient to use based on the cost-benefit analysis.

The HYDRUS-1D is a model developed by the Department of Environmental Sciences of the University of California Riverside which allows the simulation of one-dimensional water flow through a variable saturation porous medium, governed by the modified Richards's equation (Equation (6)):

$$\frac{\partial \theta}{\partial t} = \frac{\partial}{\partial z} \left[ K \left( \frac{\partial h}{\partial z} + 1 \right) \right] - S \quad (6)$$

where  $\theta$  is the volumetric water content ( $L^3 L^{-3}$ ),  $t$  is the time (T),  $h$  is the substrate water matric head (L),  $K$  is the hydraulic conductivity ( $L T^{-1}$ ),  $z$  is the vertical axis (L) and  $S$  is the sink term (L), that represents the root water uptake.

The software solves this differential equation with the finite element method linear Galerkin type. To apply it, it is necessary to discretize the space and time domains and use appropriate initial and boundary conditions.

For these simulations, the space domain has been made of a soil substrate with a thickness of 15 cm, typical of the growing medium of NBS systems, it has been divided into 100 discretization points and it has been characterized by hydraulic parameters defined from the van Genuchten unimodal (VG unimodal) model and van Genuchten bimodal (VG bimodal) model used for the definition of the SWRC and the UHCC measured by HYPROP (Tables 2 and 3).

The VG unimodal model defines the SWRC and the UHCC as follows:

$$\Theta(h) = \begin{cases} \frac{1}{[1 + (\alpha^*|h|)^n]^m} & \text{if } h \leq 0 \\ 1 & \text{if } h > 0 \end{cases} \quad (7)$$

$$K(h) = \begin{cases} K_s * \Theta^{\tau_*} \left\{ \left[ 1 - \left( 1 - \Theta^{\frac{1}{m}} \right) \right]^m \right\}^2 & \text{if } h < 0 \\ K_s & \text{if } h > 0 \end{cases} \quad (8)$$

while the VG bimodal model defines the SWRC and the UHCC as follows:

$$\Theta(h) = \begin{cases} \frac{\sum_{i=1}^2 w_i}{1} \frac{1}{[1 + (\alpha_i^*|h|)^{n_i}]^{m_i}} & \text{if } h \leq 0 \\ 1 & \text{if } h > 0 \end{cases} \quad (9)$$

$$K(h) = \begin{cases} K_s * \Theta^{\tau_*} \sum_{i=1}^2 w_i \{ [1 - (1 - \Theta^{m_i})]^{m_i} \}^2 & \text{if } h < 0 \\ K_s & \text{if } h > 0 \end{cases} \quad (10)$$

where  $\alpha$  is the inverse of pressure head at air-entry pressure head ( $L^{-1}$ ),  $n(-)$  and  $m(-)$  are shape parameters associated with the distribution of pores in the soil, linked by the relation  $m = 1 - 1/n$ ,  $\tau$  is a dimensionless tortuosity parameter (-) and  $w_i$  is the weight associated with the order of voids(-).

**Table 2** | PSC and coefficient of uniformity of Soil 1, Soil 2, Soil 3 and Soil 4

#ID	Gravel (%)	Sand (%)	Silt and clay (%)	Cu
Soil 1	71.49	23.58	4.93	28.13
Soil 2	18.71	75.17	6.12	11
Soil 3	4.50	94.12	1.38	2.88
Soil 4	63.66	28.75	7.59	50

**Table 3** | Values of the measured hydraulic parameters using van Genuchten unimodal model

Van Genuchten unimodal model					
Soil	1	2	3	4	Unit of measure
$\theta_r$	0.00	0.08	0.06	0.00	$cm^3 cm^{-3}$
$\theta_s$	0.87	0.58	0.52	0.47	$cm^3 cm^{-3}$
$\alpha$	0.16	0.07	0.16	0.03	$cm^{-1}$
$n$	1.12	1.40	1.91	1.28	-
$K_s$	5,940.3	1,092.3	10,000	273.7	$cm day^{-1}$
$\tau$	0.50	0.50	0.50	0.50	-

These parameters have been defined by the HYPROP-FIT software (Pertassek *et al.* 2015) with the aim of minimizing the root mean square error (RMSE) made on  $\Theta$  and  $K$  and the Akaike Information Criterion index (AICc) that express the quality of the fitting of the theoretical curves obtained with the VG unimodal model and the VG bimodal model with respect to the experimental points measured with Hyprop.

The RMSEs are defined as follows (11):

$$\text{RMSE}_{\Theta} = \sqrt{\frac{1}{n_p} \cdot \sum_{i=1}^{n_p} (\bar{\Theta}_i - \hat{\Theta}_i)^2}, \quad \text{RMSE}_K = \sqrt{\frac{1}{n_p} \cdot \sum_{i=1}^{n_p} (\log \bar{K}_i - \log \hat{K}_i)^2} \quad (11)$$

where  $n_p$  is the experimental points' number,  $\bar{\Theta}_i$  (or  $\bar{K}_i$ ) is the theoretical value and  $\hat{\Theta}_i$  (or  $\hat{K}_i$ ) is the measured value.

The AICc index is defined as follows (12):

$$\text{AICc} = 2 \frac{k}{n} - 2 \frac{l}{n} \quad (12)$$

where  $n$  is the experimental points' number,  $k$  is the model parameters' number and  $l$  is the logarithm of the likelihood function of the model, adopting the normal error (13):

$$l = -\frac{n}{2} \cdot \left( 1 + \ln(2\pi) + \ln \left( \frac{1}{n} \cdot \sum_{i=1}^n (\log \bar{y}_i - \log \hat{y}_i)^2 \right) \right) \quad (13)$$

where  $y_i$  is the theoretical value and  $\hat{y}_i$  is the measured value.

The time domain has been discretized using an initial time step  $\Delta_{t,i} = 0.1$  min, a minimum time step  $\Delta_{t,\min} = 0.0001$  min and a maximum time step  $\Delta_{t,\max} = 15$  min.

The initial conditions refer to initial time  $t = 0$ : they have been expressed in terms of matrix potential and it has been assumed that the porous medium was initially dry, requiring a matrix suction constant along the thickness and equal to  $-100$  cm.

The boundary conditions refer to the surfaces that delimit above ( $z = L$ ) and below ( $z = 0$ ) the porous medium: an atmospheric boundary condition was applied to the top surface (precipitation) while at the bottom surface of the domain, a seepage face boundary condition was considered assuming that the water flow through the lower surface is 0 until the matrix potential is negative, i.e. imposing that  $h_{\text{See}} = 0$ . Therefore, a seepage face boundary acts as a zero-pressure head boundary once the bottom boundary node is saturated and a no-flux boundary once unsaturated.

By providing the input data (meteorological data set) measured from the weather station, the model simulated the cumulative runoff for Soil 1, Soil 2, Soil 3 and Soil 4 using the hydraulic parameters of VG unimodal model and VG bimodal model. A summary of the boundary and initial conditions is reported in Table 1.

### 3. RESULTS AND DISCUSSIONS

#### 3.1. Particle size distribution

Figure 1 and Table 2 summarized the PSD of Soil 1, Soil 2, Soil 3 and Soil 4 and the PSC and coefficient of uniformity have been specified for each soil sample.

Based on the results presented in Table 2 and Figure 1, Soil 1 is a slightly silty and slightly clay sandy gravel very well graduated, Soil 2 is a slightly silty and slightly clay gravelly sand very well graduated, Soil 3 is a slightly gravelly sand poorly graduated and Soil 4 is a slightly silty and slightly clay sandy gravel very well graduated.

#### 3.2. Substrate hydraulic properties

The SWRC and the UHCC of the four substrates investigated are reported in Figures 2–5. The results were obtained interpolating the experimental points measured by the HYPROP device with the theoretical curve of the VG unimodal model and VG bimodal model; in agreement with Mualem (1976), to represent a more realistic pore system's distribution, the tortuosity parameter  $\tau$  has been fixed to an average value of different soil sample at 0.5. Therefore, in Tables 3 and 4, the estimated hydraulic parameters value, respectively, of VG unimodal model and VG bimodal model have been specified for each soil sample. The measured data obtained by the HYPROP device were uploaded into the HYPROP-FIT software (Pertassek *et al.* 2015) to fit the analytical

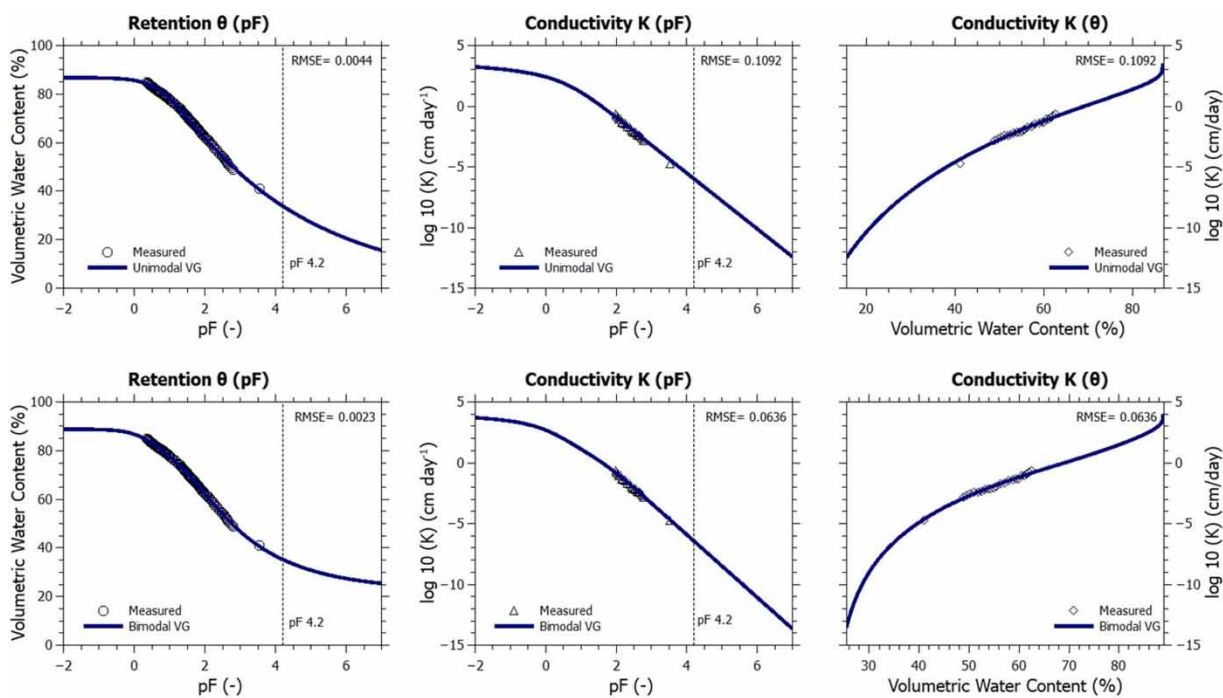


Figure 2 | SWRC and UHCC obtained using van Genuchten unimodal model and van Genuchten bimodal model for Soil 1.

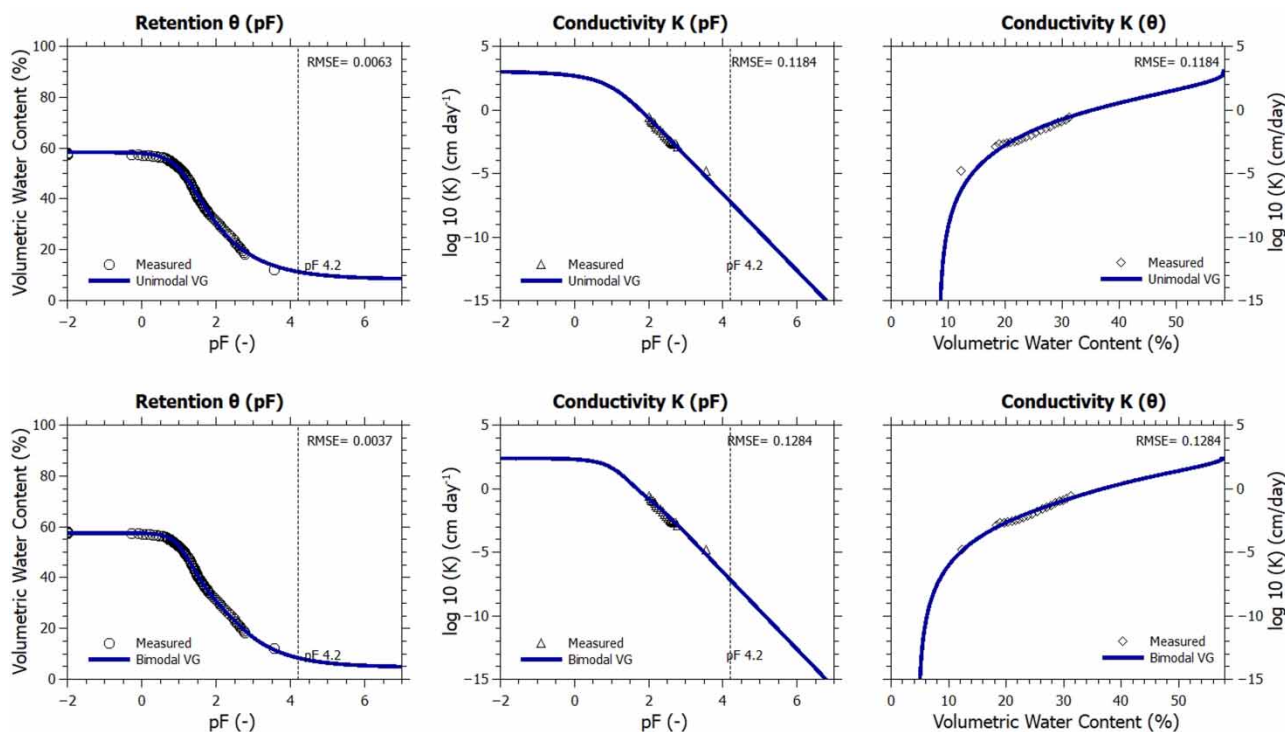


Figure 3 | SWRC and UHCC obtained using van Genuchten unimodal VG model and van Genuchten bimodal model for Soil 2.

hydraulic property functions by obtaining the best fitting with the VG unimodal model and VG bimodal model (van Genuchten 1980; Durner 1994). The measured SWRCs are well described across the whole water content range, while measured points of the hydraulic conductivity function are between 8.5 and 62% of the volumetric water content.



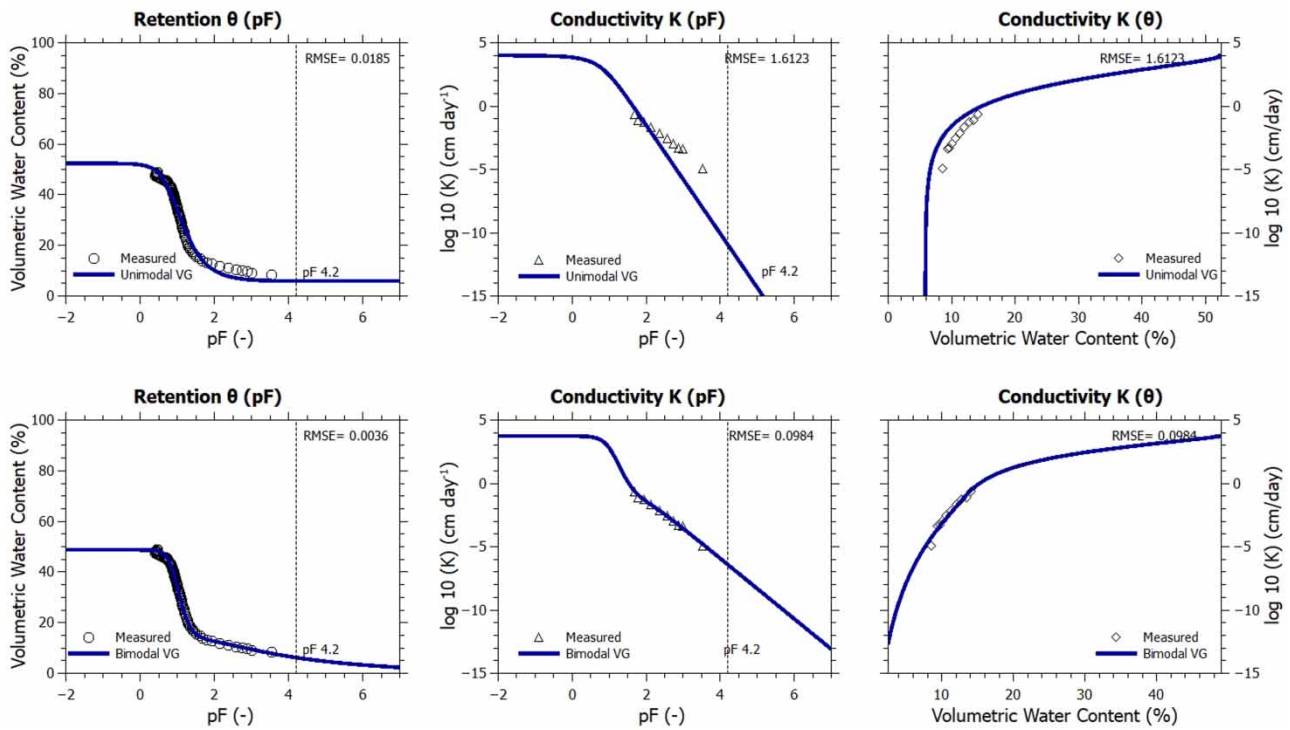


Figure 4 | SWRC and UHCC obtained using van Genuchten unimodal model and van Genuchten bimodal model for Soil 3.

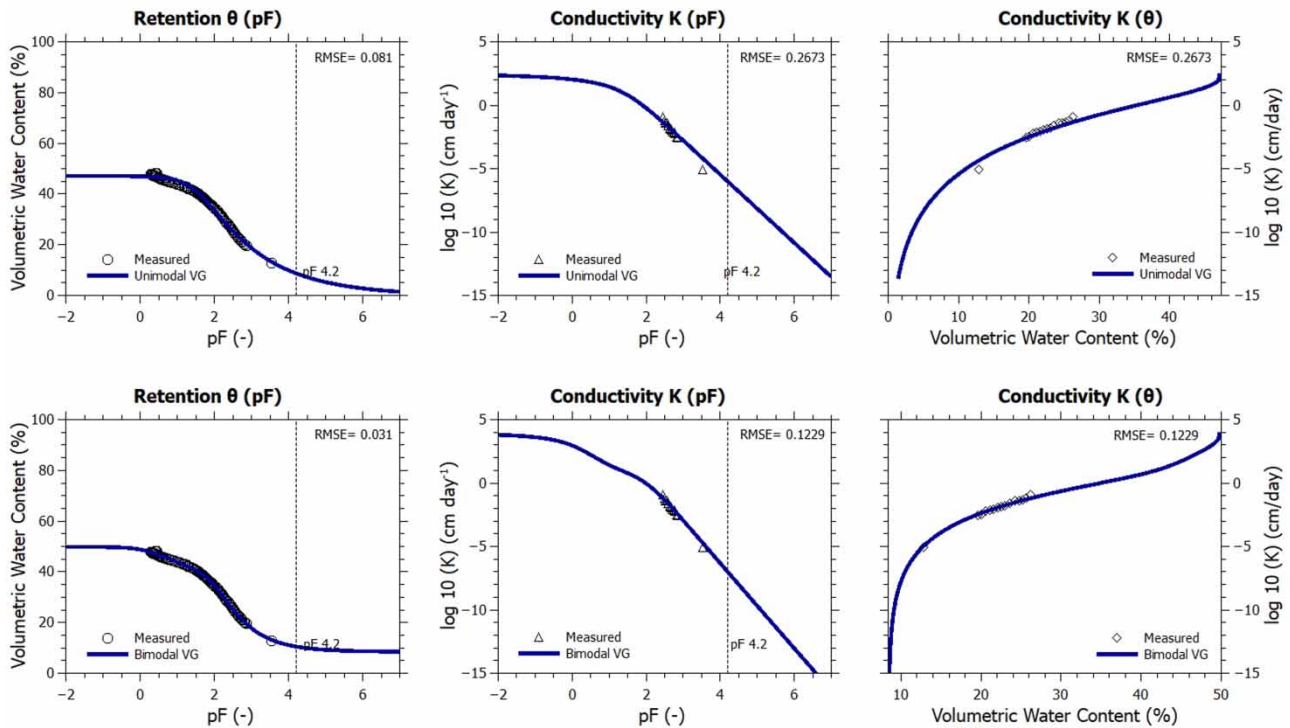


Figure 5 | SWRC and UHCC obtained using van Genuchten unimodal model and van Genuchten bimodal model for Soil 4.

**Table 4** | Values of the measured hydraulic parameters using van Genuchten bimodal model

Van Genuchten bimodal model					
Soil	1	2	3	4	Unit of measure
$\theta_r$	0.23	0.05	0.00	0.09	$\text{cm}^3 \text{cm}^{-3}$
$\theta_s$	0.89	0.58	0.49	0.50	$\text{cm}^3 \text{cm}^{-3}$
$\alpha_1$	0.5	0.01	0.10	0.01	$\text{cm}^{-1}$
$\alpha_2$	0.02	0.07	0.01	0.5	$\text{cm}^{-1}$
$n_1$	1.23	1.41	3.29	1.57	–
$n_2$	1.23	1.90	1.16	1.41	–
$w_2$	0.53	0.56	0.28	0.28	–
$K_s$	10,000	244.9	5,749.7	7,963.9	$\text{cm day}^{-1}$
$\tau$	0.50	0.50	0.50	0.50	–

Refers to VG unimodal model (Table 3), Soil 1 has the highest value of the saturated volumetric water content among all samples, thus it represents the sample with the best water capacity in saturation conditions. The shape parameters  $\alpha$  and  $n$  show, respectively, the vertical length of the transitional zone of SWRC and the slope of the back tangent to the transition zone of SWRC: the higher is  $\alpha$ 's value, the longer the transitional zone and higher is the retention capacity, i.e. in Soil 1 and Soil 3 (Figures 2 and 4), while higher is  $n$ ' value, more pendant is the transitional zone and faster is the drainage, i.e. in Soil 2 and Soil 3 (Figures 3 and 4). Regarding the values of  $K_s$ , the confidence limits obtained for this parameter are in a wide range. Thus, the huge range in the estimation of  $K_s$  shows that the evaporation method is not accurate for defining the hydraulic conductivity near saturation conditions so the use of the evaporation method to define  $K_s$  is discouraged.

Refers to VG bimodal model (Table 4), Soil 1 is confirmed as the best water content in saturation conditions. The shape parameters  $\alpha_1$ ,  $\alpha_2$ ,  $n_1$  and  $n_2$  represent, respectively, the retention's capacity in macro-pores and in micro-pores and the drainage's speed in macro-pores and in micro-pores: i.e. Soil 1 has the best retention's capacity in macro-pores and Soil 4 has the best retention's capacity in micro-pores, while Soil 3 has the best drainage's speed in macro-pores and Soil 2 has the best drainage's speed in micro-pores. As for the VG unimodal model, the estimation of  $K_s$  is not representative for the huge ranges of the confidence limits.

In soils characterized by coarse particles, the interaction between solid phase and liquid phase is mainly mechanical and this behaviour encourages the presence of macro-pores that speed the drainage processes. Thus, the transition zone of the curve develops for low values of the matrix potential. In soils characterized by fine particles, the interaction between the solid and liquid phases is mainly of an electro-chemical type (adhesion forces) and this behaviour encourages the presence of micro-pores, which slow down the drainage process. In this way, the transition zone of the curve develops for high values of the matrix potential.

The RMSE on  $\theta$  and  $K$  and the AICc index express the quality of the fitting of the theoretical curves obtained with the VG unimodal model and the VG bimodal model versus the measured points. The values of the indexes are reported in Table 5.

Comparing RMSE $_{\theta}$ , RMSE $_K$  and AICc, all the soils analysed show a bimodal hydraulic behaviour, thus their performance is better interpreted by van Genuchten bimodal model. However, for Soil 1 and Soil 2, the errors committed by VG unimodal model are contained, while for Soil 3 and Soil 4, the errors committed by VG unimodal model are gross (Table 5).

**Table 5** | Values of RMSE and AICc obtained van Genuchten unimodal model and van Genuchten bimodal model

ID	VG unimodal model			VG bimodal model		
	RMSE $_{\theta}$	RMSE $_K$	AICc	RMSE $_{\theta}$	RMSE $_K$	AICc
Soil 1	0.0044	0.1092	–1,336	0.0023	0.0636	–1,480
Soil 2	0.0063	0.1184	–1,219	0.0037	0.1284	–1,325
Soil 3	0.0185	1.6123	–815	0.0036	0.0984	–1,226
Soil 4	0.081	0.2673	–1,095	0.0031	0.1229	–1,301

This result was also expected considering that Soil 1, Soil 2, Soil 3 and Soil 4 have  $U > 2$  (Table 1), i.e. their PSC is not uniform, and this predisposes them to have a bimodal hydraulic behaviour.

In addition, the bimodality emerges especially in terms of conductivity; in fact, for all the soils analysed the error's difference on  $K$  between VG unimodal model and VG bimodal model turns out to be always greater than the error's difference that is committed to  $\theta$  between VG unimodal model and VG bimodal model.

### 3.3. Numerical modelling

Considering that all soil samples have a bimodal hydraulic behaviour, the goal of numerical modelling was to assess whether the VG bimodal model is the most convenient to use, since it depends on a greater number of parameters and therefore requires a higher computational cost. For this reason, using the same atmospheric data, the cumulative runoff was simulated using the hydraulic parameters obtained with the VG unimodal model and the VG bimodal model for Soil 1, Soil 2, Soil 3 and Soil 4 (Figure 6).

To compare the results obtained with the VG unimodal model and VG bimodal model, the relative percentage error that is made on the total volume runoff using for the substrate modelling the hydraulic parameters of VG unimodal model instead of the hydraulic parameters of the VG bimodal model (14):

$$\varepsilon = \frac{|V_{r,VGb} - V_{r,VGu}|}{V_{r,VGb}} \cdot 100 \quad (14)$$

where  $V_{r,VGu}$  is the total volume runoff obtained defining the flow domain with the use of the VG unimodal model hydraulic parameters and  $V_{r,VGb}$  is the total volume runoff obtained defining the flow domain with the use of the VG bimodal model hydraulic parameters.

In the following Table 6,  $V_{r,VGu}$ ,  $V_{r,VGb}$  and  $\varepsilon$  have been detailed for Soil 1, Soil 2, Soil 3 and Soil 4.

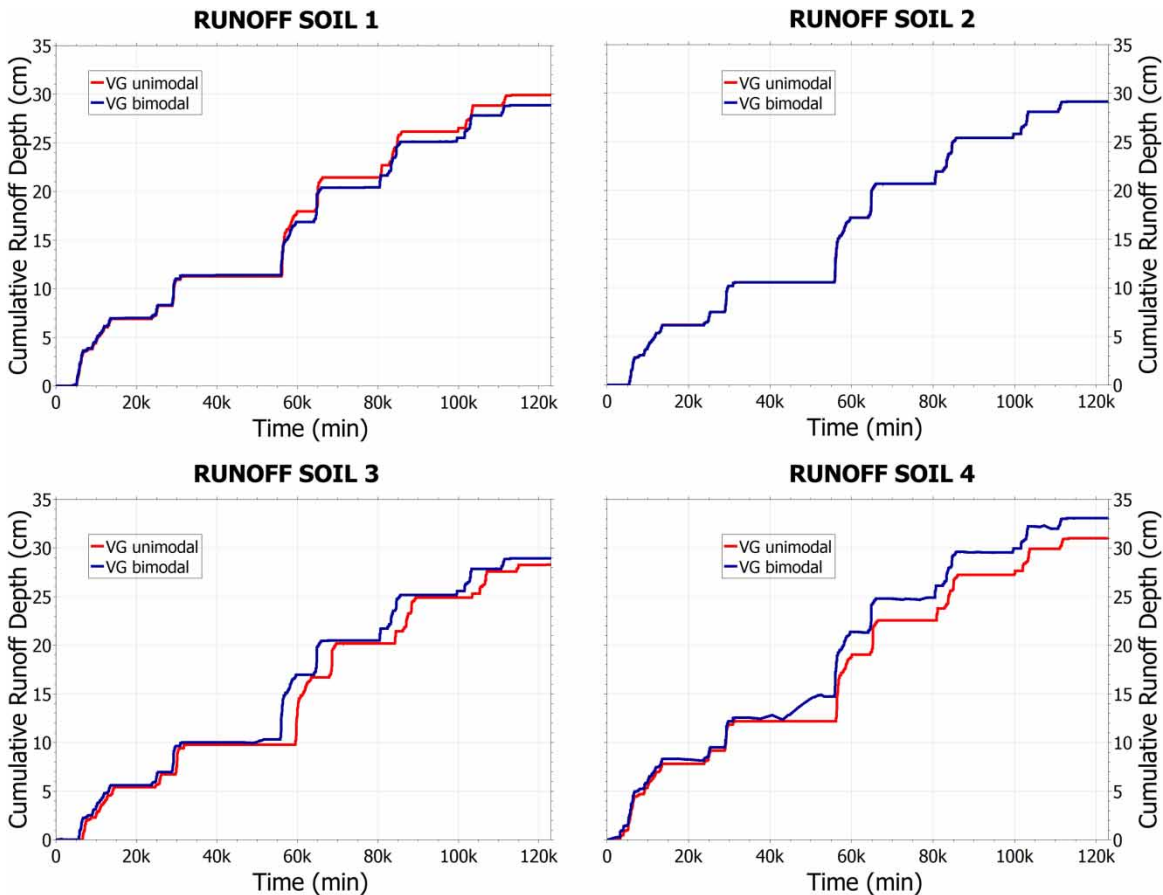


**Figure 6** | Cumulative runoff depth using van Genuchten unimodal model and van Genuchten bimodal model for Soil 1, Soil 2, Soil 3 and Soil 4.

**Table 6** | Error committed on total volume runoff using for the substrate the hydraulic parameters of VG unimodal model instead of VG bimodal model for Soil 1, Soil 2, Soil 3 and Soil 4

Soil	1	2	3	4	Unit of measure
V <sub>r</sub> (VG <sub>u</sub> )	29.91	29.16	28.66	31.00	cm
V <sub>r</sub> (VG <sub>b</sub> )	28.88	29.16	28.94	33.07	cm
$\varepsilon$	3.57	0.00	0.98	6.25	%

The results achieved show that the use of the VG unimodal model for Soil 1 overestimated the total volume runoff with respect to VG bimodal model, while for Soil 3 and Soil 4, the total volume runoff is underestimated with respect to VG bimodal model and for Soil 2, the total volume runoff is an optimal estimate. Finally, the error committed on the total runoff volume using for the substrate modelling the hydraulic parameters of the VG unimodal model instead of the hydraulic parameters of the VG bimodal model is negligible for each soil sample, as it is very low in relation to the duration of the atmospheric data observation period of three months. Although several studies show that the use of unimodal models instead of bimodal involves a loss of accuracy in hydrological simulations (Romano & Nasta 2016), our research shows that the use of the unimodal model instead of bimodal does not produce considerable errors in the runoff volume assessment that is one of the main hydrological parameters to be considered in the NBS systems. Even if Romano & Nasta (2016) assessed the benefit of using bimodal approaches in the numerical simulations of soil hydrological processes even for weak bimodality, our findings confirmed the results obtained by Brunetti *et al.* (2020). They provided a Bayesian comprehensive perspective of an NBS hydrological modelling, which included a rigorous Bayesian comparison of different Richards-based mechanistic models. The results of this study demonstrated that the unimodal van Genuchten–Mualem model is the most appropriate parameterization, and that further layers of model complexity are not fully supported by the measurements.

Our approach started from the experimental assessments of the media investigated that assured the bimodal behaviour of the substrates. Then, a simple numerical simulation, based on the hydraulic properties defined, allowed the definition of the suitability of the unimodal approach instead of the bimodal with low discrepancies.

#### 4. CONCLUSIONS

Based on the results achieved comparing the performances of the van Genuchten unimodal and bimodal models by functional evaluation of them based on the runoff from NBS substrates, we defined the following conclusion:

- The experimental investigations conducted on four NBS substrates show that their hydraulic behaviour is of bimodal type and this behaviour is even more evident in the evaluation of the unsaturated hydraulic conductivity curves than SWRC.
- The soil's hydraulic behaviour can also depend on the coefficient of uniformity's value: higher is this coefficient ( $U > 2$ ), higher is the heterogeneity of the composition, due to which the structure of the soil is defined by a double order of voids that causes its bimodal hydraulic behaviour.
- The benefit of using the unimodal model in numerical simulations of soil hydrological processes is acceptable considering that the errors in using this model instead of the bimodal for four different soils, is less than 10%. The VG unimodal model is very widespread and easy to implement while the bimodal requires extra parameters that can increase the uncertainty in the model parameters estimation. In addition, based on the results achieved during the experimental investigations (RMSE, AIC), we expected a low value of the error, during the numerical simulation with the use of the VG unimodal model, on Soil 1 and Soil 2 rather than Soil 3 and Soil 4 but we obtained larger errors on Soil 1 and Soil 4. This behaviour may be due to the analysis of the coefficient of uniformity. Soil 1 and Soil 4 have  $U > 25$ , so they are expected to behave distinctly bimodal, while Soil 2 and Soil 3 have  $U < 25$ , so they are expected to behave less obviously bimodal: in fact, the relative percentage error that is committed on the total volume runoff using the substrate hydraulic parameters of VG unimodal model instead of that of VG bimodal model for Soils 1 and Soil 4 is greater than the errors committed for Soil 2 and Soil 3. In contrast, the biggest errors were made on Soil 1 and Soil 4 compared to Soil 2 and Soil 3. A possible explanation can be sought in the analysis of the coefficient of uniformity (Table 1). Soil 1 and Soil 4 have  $U > 25$ , so they are expected to behave distinctly bimodal, while Soil 2 and Soil 3 have  $U < 25$ , so they are expected to behave less obviously bimodal: in fact, the relative percentage error that is committed on the total volume runoff using the substrate hydraulic

parameters of VG unimodal model instead of that of VG bimodal model for Soil 1 and Soil 4 is greater than the errors committed for Soil 2 and Soil 3.

Further investigation on the sensitivity of the hydraulic and physical parameters of NBS substrates investigated should be carried out to improve the knowledge of the modelling of the NBS systems as well as the effects of the root plants on the hydraulic behaviour.

## ACKNOWLEDGEMENTS

The experimental investigation and the numerical analysis were carried out during the “TOP FREE - Tetti e Orti Pensili a “Fileria corta” per la Riqualificazione di Edifici Esistenti” - POR CALABRIA FESR-FSE 2014–2020 - Action 1.1.5- CUP J29J21001760005 and during the national project “PRIN 2020 - URCA!” supported by Italian Ministry for University and Research. The author Stefania Anna Palermo WAS supported by the Italian Ministry for University and Research (D.M. n. 1062/2021) - REACT EU - National Operational Program on Research and Innovation (PON R&I) 2014–2020 – Axis IV; Action IV.4, Action IV.6. CUP: H25F21001230004. IC: 1062\_R18\_GREEN. The author Ludovica Presta WAS supported by the Italian Ministry for University and Research (D.M. n. 1061/2021) - National Operational Program on Research and Innovation (PON R&I) 2014–2020. Research Doctorates on Green and Innovation issues.

## DATA AVAILABILITY STATEMENT

All relevant data are included in the paper or its Supplementary Information.

## CONFLICT OF INTEREST

The authors declare there is no conflict.

## REFERENCES

- Arnold, C. L. & Gibbons, C. J. 1996 **Impervious surface coverage: The emergence of a key environmental indicator**. *Journal of the American Planning Association* **62** (2), 243–258.
- ASTM D2487 2000 D2487: standard practice for classification of soils for engineering purposes (Unified Soil Classification System). *ASTM International* **04**, 1–12.
- Brewer, R. 1965 **Fabric and mineral analysis of soils**. *Soil Science* **100** (1), 73.
- Brunetti, G., Šimůnek, J. & Piro, P. 2016 **A comprehensive analysis of the variably saturated hydraulic behavior of a green roof in a Mediterranean climate**. *Vadose Zone Journal* **15** (9), 1–17.
- Brunetti, G., Papagrorgiou, I. A. & Stumpp, C. 2020 **Disentangling model complexity in green roof hydrological analysis: A Bayesian perspective**. *Water Research* **182**, 115973. <https://doi.org/10.1016/j.watres.2020.115973>.
- Carbone, M., Turco, M., Nigro, G. & Piro, P. 2014 **Modeling of hydraulic behaviour of green roof in catchment scale**. In *International Multidisciplinary Scientific GeoConference Surveying Geology and Mining Ecology Management, SGEM*.
- Coppola, A. 2000 **Unimodal and bimodal descriptions of hydraulic properties for aggregated soils**. *Soil Science Society of America Journal* **64** (4), 1252–1262.
- Coppola, A., Basile, A., Comegna, A. & Lamaddalena, N. 2009 **Monte Carlo analysis of field water flow comparing uni- and bimodal effective hydraulic parameters for structured soil**. *Journal of Contaminant Hydrology* **104** (1–4), 153–165.
- Costa-Conceicao, K., Villamar Ayala, C. A., Dávila, T. & Gallardo, M. C. 2023 **Performance of hybrid biofilter based on rice husks/sawdust treating grey wastewater**. *Water Science and Technology: A Journal of the International Association on Water Pollution Research* **87** (10), 2416–2431.
- Dexter, A. R. 1988 **Advances in characterization of soil structure**. *Soil and Tillage Research* **11** (3–4), 199–238.
- Dexter, A. R., Czyz, E. A., Richard, G. & Reszkowska, A. 2008 **A user-friendly water retention function that takes account of the textural and structural pore spaces in soil**. *Geoderma* **143** (3–4), 243–253.
- Durner, W. 1994 **Hydraulic conductivity estimation for soils with heterogeneous pore structure**. *Water Resources Research* **30** (2), 211–223.
- Espey, W. H. J., Morgan, C. W. & Masch, F. D. (1964) *Study of Some Effects of Urbanization on Storm Runoff from a Small Watershed*. Available from: [https://www.twdb.texas.gov/publications/reports/numbered\\_reports/doc/R23/R23.pdf](https://www.twdb.texas.gov/publications/reports/numbered_reports/doc/R23/R23.pdf), <https://repositories.lib.utexas.edu/handle/2152/64863>.
- Falconer, R. H., Cobby, D., Smyth, P., Astle, G., Dent, J. & Golding, B. 2009 **Pluvial flooding: New approaches in flood warning, mapping and risk management**. *Journal of Flood Risk Management* **2** (3), 198–208.
- Finkenbine, J. K., Atwater, J. W. & Mavinic, D. S. 2000 **Stream health after urbanization**. *Journal of the American Water Resources Association* **36** (5), 1149–1160.

- Fletcher, T. D., Andrieu, H. & Hamel, P. 2013 Understanding, management and modelling of urban hydrology and its consequences for receiving waters: A state of the art. *Advances in Water Resources* **51**, 261–279.
- Hadas, A. 1987 Long-term tillage practice effects on soil aggregation modes and strength. *Soil Science Society of America Journal* **51** (1), 191–197.
- Kumar, S. & Singh, K. K. 2023 Hydrological performance of rain gardens having *Calendula officinalis* plant with varied planting mixtures. *Water Science and Technology* **87** (5), 1316–1326.
- Kutilek, M. 2004 Soil hydraulic properties as related to soil structure. *Soil and Tillage Research* **79** (2), 175–184.
- Leopold, L. 1968 Hydrology for urban land planning – a guidebook on the hydrologic effects of urban land use. *Geological Survey Circular* **554**, 1–21. Available from: <http://enviro.lclark.edu/resources/Tryon/Water/Hydrology.pdf>.
- Masi, F., Bresciani, R., Rizzo, A., Edathoot, A., Patwardhan, N., Panse, D. & Langergraber, G. 2016 Green walls for greywater treatment and recycling in dense urban areas: A case-study in Pune. *Journal of Water Sanitation and Hygiene for Development* **6** (2), 342–347.
- Masson-Delmotte, V., Zhai, P., Pirani, A., Connors, S. L., Péan, C., Berger, S., Caud, N., Chen, Y., Goldfarb, L., Gomis, M. I., Huang, M., Leitzell, K., Lonnoy, E., Matthews, J. B. R., Maycock, T. K., Waterfield, T., Yelekçi, O., Yu, R. & Zhou, B. 2021 *IPCC, 2021: Climate Change 2021: The Physical Science Basis*. Available from: <https://www.ipcc.ch/report/ar6/wg1/>.
- METER 2015 Hyprop 2. HYPROP Manual. Available from: [www.link.com](http://www.link.com).
- Monterusso, M. A., Rowe, D. B., Rugh, C. L. & Russell, D. K. 2004 Runoff water quantity and quality from green roof systems. *Acta Horticulturae* **639**, 369–376.
- Mualem, Y. 1976 A new model for predicting the hydraulic conductivity of unsaturated porous media. *Water Resources Research* **12** (3), 513–522.
- Oades, J. M. & Waters, A. G. 1991 Aggregate hierarchy in soils. *Australian Journal of Soil Research* **29** (6), 815–825.
- Palermo, S. A., Zischg, J., Sitzenfrei, R., Rauch, W. & Piro, P. 2019 Parameter sensitivity of a microscale hydrodynamic model. In *Green Energy and Technology*.
- Palermo, S. A., Talarico, V. C. & Turco, M. 2020 On the LID systems effectiveness for urban stormwater management: Case study in Southern Italy. *IOP Conference Series: Earth and Environmental Science* **410**, 012012.
- Penny, J., Alves, P. B. R., De-Silva, Y., Chen, A. S., Djordjević, S., Shrestha, S. & Babel, M. 2023 Analysis of potential nature-based solutions for the Mun River Basin, Thailand. *Water Science and Technology* **87** (6), 1496–1514.
- Pertassek, T., Peters, A. & Durner, W. 2015 HYPROP-FIT User's Manual., (V.3.0), 66.
- Peters, A. & Durner, W. 2008 Simplified evaporation method for determining soil hydraulic properties. *Journal of Hydrology* **356** (1–2), 147–162.
- Pirouz, B., Turco, M. & Palermo, S. A. 2020 A novel idea for improving the efficiency of green walls in urban environment (an innovative design and technique). *Water (Switzerland)* **12** (12), 1–16.
- Richards, L. A. 1931 Capillary conduction of liquids through porous mediums. *Journal of Applied Physics* **1** (5), 318–333.
- Romano, N. & Nasta, P. 2016 How effective is bimodal soil hydraulic characterization? Functional evaluations for predictions of soil water balance. *European Journal of Soil Science* **67** (4), 523–535.
- Rose, S. & Peters, N. E. 2001 Effects of urbanization on streamflow in the Atlanta area (Georgia, USA): A comparative hydrological approach. *Hydrological Processes* **15** (8), 1441–1457.
- Ross, P. J. & Smettem, K. R. J. 1993 Describing soil hydraulic properties with sums of simple functions. *Soil Science Society of America Journal* **57** (1), 26–29.
- Salerno, F., Valsecchi, L., Minoia, R., Copetti, D., Tartari, G., Guyennon, N., Colombo, N., Pirola, N., Barozzi, B., Bellazzi, A. & Marziali, L. 2021 Factors controlling the hydraulic efficiency of green roofs in the metropolitan area of Milan (Italy). *Sustainability (Switzerland)* **13** (24), 1–13.
- Schaap, M. G. & Leij, F. J. 1998 Database-related accuracy and uncertainty of pedotransfer functions. *Soil Science* **163** (10), 765–779.
- Schindler, U. 1980 *Ein Schnellverfahren zur Messung der Wasserleitfähigkeit im Teilgesättigten Boden an Stechzylinderproben*.
- Schindler, U., Durner, W., von Unold, G., Mueller, L. & Wieland, R. 2010a The evaporation method: Extending the measurement range of soil hydraulic properties using the air-entry pressure of the ceramic cup. *Journal of Plant Nutrition and Soil Science* **173** (4), 563–572.
- Schindler, U., Durner, W., von Unold, G. & Muller, L. 2010b Evaporation method for measuring unsaturated hydraulic properties of soils: Extending the measurement range. *Soil Science Society of America Journal* **74** (4), 1071–1083.
- Sims, A. W., Robinson, C. E., Smart, C. C. & O'Carroll, D. M. 2019 Mechanisms controlling green roof peak flow rate attenuation. *Journal of Hydrology* **577**, 1–13.
- Šimůnek, J., van Genuchten, M. T. & Šejna, M. 2016 Recent developments and applications of the HYDRUS computer software packages. *Vadose Zone Journal* **15** (7), 1–25.
- Stovin, V., Vesuviano, G. & De-Ville, S. 2017 Defining green roof detention performance. *Urban Water Journal* **14** (6), 574–588.
- Turco, M., Brunetti, G., Carbone, M. & Piro, P. 2018 Modelling the hydraulic behaviour of permeable pavements through a reservoir element model. In *International Multidisciplinary Scientific GeoConference Surveying Geology and Mining Ecology Management, SGEM*.
- Turco, M., Brunetti, G., Palermo, S. A., Capano, G., Grossi, G., Maiolo, M. & Piro, P. 2020 On the environmental benefits of a permeable pavement: Metals potential removal efficiency and life cycle assessment. *Urban Water Journal* **00** (00), 1–9. <https://doi.org/10.1080/1573062X.2020.1713380>.

- Turco, M., Palermo, S. A., Maiolo, M., Pirouz, B. & Piro, P. 2022 Experimental and numerical analysis to assess the substrate hydraulic properties and the retention capacity of a green wall module. *Urban Water Journal* **00** (00), 1–11. <https://doi.org/10.1080/1573062X.2022.2138461>.
- van Genuchten, M. T. 1980 A closed-form equation for predicting the hydraulic conductivity of unsaturated soils. *Soil Science Society of America Journal* **44** (5), 892–898.
- Vervoort, R. W. & Cattle, S. R. 2003 Linking hydraulic conductivity and tortuosity parameters to pore space geometry and pore-size distribution. *Journal of Hydrology* **272** (1–4), 36–49.
- Wang, J., Garg, A., Huang, S., Mei, G., Liu, J., Zhang, K. & Gan, L. 2021 The rainwater retention mechanisms in extensive green roofs with ten different structural configurations. *Water Science and Technology* **84** (8), 1839–1857.
- Wind, G. P. 1969 Capillary conductivity data estimated by a simple method. In *Water in the Unsaturated Zone, Proceedings of Wageningen Symposium*.
- Wösten, J. H. M., Finke, P. A. & Jansen, M. J. W. 1995 Comparison of class and continuous pedotransfer functions to generate soil hydraulic characteristics. *Geoderma* **66** (3–4), 227–237.
- Zhang, Y., Weihermüller, L., Toth, B., Noman, M. & Vereecken, H. 2022 Analyzing dual porosity in soil hydraulic properties using soil databases for pedotransfer function development. *Vadose Zone Journal* **21** (5), 1–21.

First received 16 March 2023; accepted in revised form 14 July 2023. Available online 26 July 2023